

Multi-Tubal Rank of Third Order Tensor and Related Low Rank Tensor Completion Problem

Xinzen Zhang

Tianjin University

2020.12.18

Joint work with Quan Yu and Zheng-Hai Huang

Contents

- 1 Introduction
- 2 Multi-tubal rank: Definition and motivation
- 3 Tensor completion problem based on multi-tubal rank
- 4 Improvement with spatio-temporal characteristics
- 5 Numerical examples

Contents

- 1 Introduction
- 2 Multi-tubal rank: Definition and motivation
- 3 Tensor completion problem based on multi-tubal rank
- 4 Improvement with spatio-temporal characteristics
- 5 Numerical examples

Definition (Tensor)

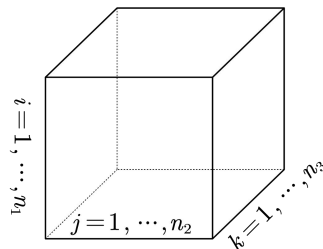
A tensor is a multidimensional array. More formally, an N -way or N th-order tensor is an element of the tensor product of N vector spaces, each of which has its own coordinate system.



A first order tensor (vector)



A second order tensor (matrix)



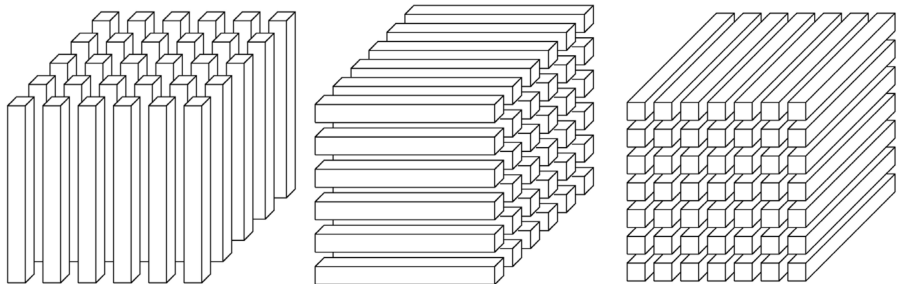
A third order tensor: $\mathcal{X} \in \mathbb{R}^{n_1 \times n_2 \times n_3}$

Figure: tensor.

Fibers

Definition (Fibers)

Fibers are the higher-order analogue of matrix rows and columns. A fiber is defined by fixing every index but one.



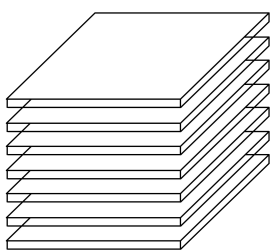
(a) Mode-1 (col) fibers: $x_{:jk}$ (b) Mode-2 (row) fibers: $x_{i:k}$ (c) Mode-3 (tube) fibers: $x_{ij:}$

Figure: Fibers of a 3rd-order tensor.

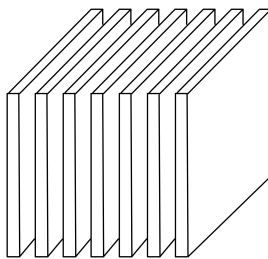
Slices

Definition (Slices)

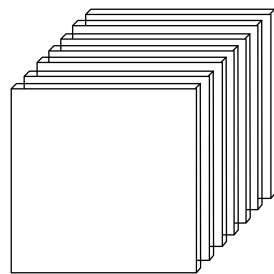
Slices are two-dimensional sections of a tensor, defined by fixing all but two indices.



(a) Horizontal slices: $X_{i::}$



(b) Lateral slices: $X_{::j}$



(c) Frontal slices: $X_{::k}$

Figure: Slices of a 3rd-order tensor.

CANDECOMP/PARAFAC Decomposition

Definition (CP Decomposition)

Suppose that $\mathcal{X} \in \mathbb{R}^{n_1 \times n_2 \times \cdots \times n_m}$. If there exist $a_r^{(i)} \in \mathbb{R}^{n_i}$ for $i = 1, \dots, m$ such that

$$\mathcal{X} = \sum_{r=1}^R a_r^{(1)} \circ a_r^{(2)} \circ \cdots \circ a_r^{(m)}, \quad a_r^{(k)} \in \mathbb{R}^{n_k}. \quad (1)$$

The (1) is said to be a CP decomposition of \mathcal{X} . The smallest R of (1) is called CP-rank, denoted by $rank_{CP}(\mathcal{X})$. The CP decomposition with $R = rank_{CP}(\mathcal{X})$ is called a CP rank decomposition.

Remark: It is NP-hard to determine CP rank.

Tucker rank

Definition

For a tensor $\mathcal{X} \in \mathbb{R}^{n_1 \times n_2 \cdots \times n_m}$, let $X_{(i)} \in n_i \times N_i$ for $i \in [m]$. The Tucker rank (or n -rank) of \mathcal{X} is

$$\text{rank}_{tc}(\mathcal{X}) = (\text{rank}(X_{(1)}), \dots, \text{rank}(X_{(m)})) ,$$

where $N_i = n_1 \times \cdots \times n_{i-1} \times n_{i+1} \times \cdots \times n_m$.

Tubal rank

For $\mathcal{A} \in \mathbb{R}^{n_1 \times n_2 \times n_3}$, let $\bar{\mathcal{A}} \in \mathbb{C}^{n_1 \times n_2 \times n_3}$ be the result of Discrete Fourier transformation (DFT) of $\mathcal{A} \in \mathbb{R}^{n_1 \times n_2 \times n_3}$ along the mode-3. Specifically, let $F_{n_3} = [\mathbf{f}_1, \dots, \mathbf{f}_{n_3}] \in \mathbb{C}^{n_3 \times n_3}$, where

$$\mathbf{f}_i = \left[\omega^{0 \times (i-1)}, \omega^{1 \times (i-1)}, \dots, \omega^{(n_3-1) \times (i-1)} \right] \in \mathbb{C}^{n_3}$$

with $\omega = e^{-\frac{2\pi i}{n_u}}$ and $i = \sqrt{-1}$. Let

$$\bar{\mathcal{A}}_3(i, j, :) = F_{n_3} \mathcal{A}(i, j, :),$$

which can be computed by Matlab command “ $\bar{\mathcal{A}}_u = fft(\mathcal{A}, [], u)$ ”. Furthermore, \mathcal{A} can be computed by $\bar{\mathcal{A}}_u$ with the inverse DFT $\mathcal{A} = ifft(\bar{\mathcal{A}}_u, [], u)$.

Definition

For any tensor $\mathcal{A} \in \mathbb{R}^{n_1 \times n_2 \times n_3}$, let $r^l = \text{rank}(\bar{\mathcal{A}}^{(l)})$ and $l \in [\mathbf{n}_3]$. Then tubal rank of \mathcal{A} is defined as $\text{rank}_t(\mathcal{A}) = \max\{r^1, r^2, \dots, r^{n_3}\}$.

Tensor Completion

Low rank tensor completion:

$$\min_{\mathcal{C}} \text{rank}(\mathcal{C}) \quad \text{s.t.} \quad P_{\Omega}(\mathcal{C}) = P_{\Omega}(\mathcal{M}),$$

where $\text{rank}(\cdot)$ is a tensor rank and Ω is an index set locating the observed data. P_{Ω} is a linear operator that extracts the entries in Ω and fills the entries not in Ω with zeros, and \mathcal{M} is a given tensor.

Based on tubal rank, tensor completion based on tensor factorization was considered

$$\min_{\mathcal{X}, \mathcal{Y}, \mathcal{C}} \frac{1}{2} \|\mathcal{X} * \mathcal{Y} - \mathcal{C}\|_F^2, \quad \text{s.t.} \quad P_\Omega(\mathcal{C} - \mathcal{M}) = 0, \quad (2)$$

where “*” denotes the t-product. By analysis, the t-product can be computed by some block diagonal matrices of smaller sizes, which makes a significant reduction of computational cost.

Contents

- 1 Introduction
- 2 Multi-tubal rank: Definition and motivation
- 3 Tensor completion problem based on multi-tubal rank
- 4 Improvement with spatio-temporal characteristics
- 5 Numerical examples

Discrete Fourier Transformation (DFT)

For $\mathcal{A} \in \mathbb{R}^{n_1 \times n_2 \times n_3}$ and $u \in [3]$, let $\bar{\mathcal{A}}_u \in \mathbb{C}^{n_1 \times n_2 \times n_3}$ be the result of Discrete Fourier transformation (DFT) of $\mathcal{A} \in \mathbb{R}^{n_1 \times n_2 \times n_3}$ along the u -th mode. Specifically, let $F_{n_u} = [\mathbf{f}_1, \dots, \mathbf{f}_{n_u}] \in \mathbb{C}^{n_u \times n_u}$, where

$$\mathbf{f}_i = \left[\omega^{0 \times (i-1)}; \omega^{1 \times (i-1)}; \dots; \omega^{(n_u-1) \times (i-1)} \right] \in \mathbb{C}^{n_u}$$

with $\omega = e^{-\frac{2\pi i}{n_u}}$ and $i = \sqrt{-1}$. Then

$$\bar{\mathcal{A}}_1(:, j, k) = F_{n_1} \mathcal{A}(:, j, k), \quad \bar{\mathcal{A}}_2(i, :, k) = F_{n_2} \mathcal{A}(i, :, k), \quad \bar{\mathcal{A}}_3(i, j, :) = F_{n_3} \mathcal{A}(i, j, :),$$

which can be computed by Matlab command “ $\bar{\mathcal{A}}_u = fft(\mathcal{A}, [], u)$ ”. Furthermore, \mathcal{A} can be computed by $\bar{\mathcal{A}}_u$ with the inverse DFT $\mathcal{A} = ifft(\bar{\mathcal{A}}_u, [], u)$.

Generalized T_u -product and multi-tubal rank

For \mathcal{A} , we define matrices \bar{A}_1 , \bar{A}_2 and \bar{A}_3 as

$$\bar{A}_u = bdiag_u(\bar{\mathcal{A}}_u) = \begin{bmatrix} \bar{A}_u^{(1)} & & & \\ & \bar{A}_u^{(2)} & & \\ & & \ddots & \\ & & & \bar{A}_u^{(n_u)} \end{bmatrix}, \quad \forall u \in [3].$$

The block circulant matrices $bcirc_1(\mathcal{A})$, $bcirc_2(\mathcal{A})$ and $bcirc_3(\mathcal{A})$ of \mathcal{A} are defined as

$$bcirc_u(\mathcal{A}) = \begin{bmatrix} A_u^{(1)} & A_u^{(n_u)} & \dots & A_u^{(2)} \\ A_u^{(2)} & A_u^{(1)} & \dots & A_u^{(3)} \\ \vdots & \vdots & \ddots & \vdots \\ A_u^{(n_u)} & A_u^{(n_u-1)} & \dots & A_u^{(1)} \end{bmatrix}, \quad \forall u \in [3].$$

Definition (Generalized \mathcal{T}_u -product)

For $\mathcal{A}_1 \in \mathbb{R}^{n_1 \times n_2 \times r_1}$ and $\mathcal{B}_1 \in \mathbb{R}^{n_1 \times r_1 \times n_3}$, define

$$\mathcal{A}_1 *_1 \mathcal{B}_1 := \text{fold}_1(\text{bcirc}_1(\mathcal{A}_1) \cdot \text{unfold}_1(\mathcal{B}_1)) \in \mathbb{R}^{n_1 \times n_2 \times n_3}.$$

For $\mathcal{A}_2 \in \mathbb{R}^{n_1 \times n_2 \times r_2}$ and $\mathcal{B}_2 \in \mathbb{R}^{r_2 \times n_2 \times n_3}$, define

$$\mathcal{A}_2 *_2 \mathcal{B}_2 := \text{fold}_2(\text{bcirc}_2(\mathcal{A}_2) \cdot \text{unfold}_2(\mathcal{B}_2)) \in \mathbb{R}^{n_1 \times n_2 \times n_3}.$$

For $\mathcal{A}_3 \in \mathbb{R}^{n_1 \times r_3 \times n_3}$ and $\mathcal{B}_3 \in \mathbb{R}^{r_3 \times n_2 \times n_3}$, define

$$\mathcal{A}_3 *_3 \mathcal{B}_3 := \text{fold}_3(\text{bcirc}_3(\mathcal{A}_3) \cdot \text{unfold}_3(\mathcal{B}_3)) \in \mathbb{R}^{n_1 \times n_2 \times n_3}.$$

Here

$$\text{unfold}_u(\mathcal{B}_u) = [B_u^{(1)}; B_u^{(2)}; \dots; B_u^{(n_u)}],$$

and its inverse operator “ fold_u ” is defined by $\text{fold}_u(\text{unfold}_u(\mathcal{B}_u)) = \mathcal{B}_u$.

Definition (Multi-tubal rank)

For any tensor $\mathcal{A} \in \mathbb{R}^{n_1 \times n_2 \times n_3}$ and $u \in [3]$, let $r_u^l = \text{rank}(\bar{\mathcal{A}}_u^{(l)})$ and $l \in [\mathbf{n}_u]$. Then multi-tubal rank of \mathcal{A} is defined as

$$\text{rank}_{mt}(\mathcal{A}) = (r_1(\mathcal{A}), r_2(\mathcal{A}), r_3(\mathcal{A})),$$

where $r_u(\mathcal{A}) = \max\{r_u^1, r_u^2, \dots, r_u^{n_u}\}$ for $u \in [3]$.

In fact, the T_3 -product is the classical t -product and $r_3(\mathcal{A})$ is tubal rank of tensor \mathcal{A} , respectively.

Lemma

For given $u \in [3]$, suppose that \mathcal{A}, \mathcal{B} are tensors such that $\mathcal{A} *_u \mathcal{B}$ is well defined, and $\mathcal{F} = \mathcal{A} *_u \mathcal{B}$ is defined as in Definition 7. Then,

- (1) $\|\mathcal{A}\|_F^2 = \frac{1}{n_u} \|\bar{\mathcal{A}}_u\|_F^2$;
- (2) $\mathcal{F} = \mathcal{A} *_u \mathcal{B}$ and $\bar{\mathcal{F}}_u = \bar{\mathcal{A}}_u \bar{\mathcal{B}}_u$ are equivalent;
- (3) $r_u(\mathcal{F}) \leq \min\{r_u(\mathcal{A}), r_u(\mathcal{B})\}$.

From Lemma 9, we can assert that the generalized tensor factorization can be computed by matrix factorization, which is computable.

Motivation of multi-tubal rank

Lemma

Suppose that $\mathcal{C} \in \mathbb{R}^{n_1 \times n_2 \times n_3}$ is a tensor and $F \in \mathbb{R}^{n_1 \times n_1}$, $G \in \mathbb{R}^{n_2 \times n_2}$, $H \in \mathbb{R}^{(n_3-1) \times n_3}$ are three matrices. Then

$$\mathcal{F} *_2 \mathcal{C} = \mathcal{C} \times_1 F, \quad \mathcal{C} *_3 G = \mathcal{C} \times_2 G, \quad \mathcal{C} *_1 H = \mathcal{C} \times_3 H,$$

where

$$\mathcal{F} \in \mathbb{R}^{n_1 \times n_2 \times n_1}, \quad \mathcal{G} \in \mathbb{R}^{n_2 \times n_2 \times n_3}, \quad \mathcal{H} \in \mathbb{R}^{n_1 \times n_3 \times (n_3-1)},$$

$$F_2^{(1)} = F, \quad F_2^{(2)} = \cdots = F_2^{(n_2)} = 0,$$

$$G_3^{(1)} = G^T, \quad G_3^{(2)} = \cdots = G_3^{(n_3)} = 0,$$

$$H_1^{(1)} = H^T, \quad H_1^{(2)} = \cdots = H_1^{(n_1)} = 0.$$

The relationship between Tucker rank and multi-tubal rank

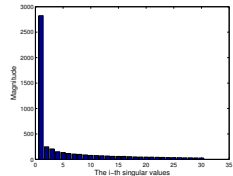
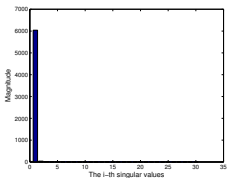
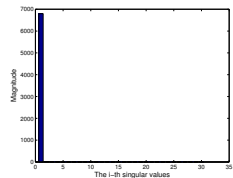
Theorem

For any tensor $\mathcal{A} = (\mathcal{A}_{ijk}) \in \mathbb{R}^{n_1 \times n_2 \times n_3}$, the following properties hold:

$$\begin{aligned} r_1(\mathcal{A}) &\leq \min \left\{ r(A_{(2)}), r(A_{(3)}) \right\}, \\ r_2(\mathcal{A}) &\leq \min \left\{ r(A_{(1)}), r(A_{(3)}) \right\}, \\ r_3(\mathcal{A}) &\leq \min \left\{ r(A_{(1)}), r(A_{(2)}) \right\}. \end{aligned}$$



(a) Sampled frames in video

(b) The first 30 singular values of $\bar{A}_3^{(1)}$ (c) The singular values of $\bar{A}_1^{(1)}$ (d) The singular values of $\bar{A}_2^{(1)}$ Figure: The sampled frames in video and singular values of $\bar{A}_u^{(1)}$ for $u \in [3]$

Contents

- 1 Introduction
- 2 Multi-tubal rank: Definition and motivation
- 3 Tensor completion problem based on multi-tubal rank
- 4 Improvement with spatio-temporal characteristics
- 5 Numerical examples

Based on the introduced multi-tubal rank, the tensor completion problem can be modeled as:

$$\min_{\mathcal{C} \in \mathbb{R}^{n_1 \times n_2 \times n_3}} \text{rank}_{mt}(\mathcal{C}), \quad \text{s.t.} \quad P_{\Omega}(\mathcal{C} - \mathcal{M}) = 0, \quad (3)$$

which is a vector optimization problem. To simplify the computation, we consider the following single objective optimization problem

$$\min_{\mathcal{C} \in \mathbb{R}^{n_1 \times n_2 \times n_3}} \sum_{u=1}^3 \alpha_u r_u(\mathcal{C}), \quad \text{s.t.} \quad P_{\Omega}(\mathcal{C} - \mathcal{M}) = 0,$$

where $\alpha_1, \alpha_2, \alpha_3 \geq 0$ and $\sum_{u=1}^3 \alpha_u = 1$.

Note that \mathcal{C} can be factorized as $\mathcal{C} = \mathcal{X}_u *_u \mathcal{Y}_u$ with $r_u(\mathcal{C}) \leq \min(r_u(\mathcal{X}_u), r_u(\mathcal{Y}_u))$ for $u \in [3]$. Hence we consider the following tensor factorization model

$$\min_{\mathcal{C}, \mathcal{X}_u, \mathcal{Y}_u} \sum_{u=1}^3 \frac{\alpha_u}{2} \|\mathcal{X}_u *_u \mathcal{Y}_u - \mathcal{C}\|_F^2 \quad \text{s.t.} \quad P_\Omega(\mathcal{C} - \mathcal{M}) = 0$$

with its regularized model

$$\min_{\mathcal{C}, \mathcal{X}_u, \mathcal{Y}_u} f(\mathcal{C}, \mathcal{X}_1, \mathcal{X}_2, \mathcal{X}_3, \mathcal{Y}_1, \mathcal{Y}_2, \mathcal{Y}_3) \quad \text{s.t.} \quad P_\Omega(\mathcal{C} - \mathcal{M}) = 0. \quad (4)$$

Here,

$$\begin{aligned} f(\mathcal{C}, \mathcal{X}_1, \mathcal{X}_2, \mathcal{X}_3, \mathcal{Y}_1, \mathcal{Y}_2, \mathcal{Y}_3) \\ = \sum_{u=1}^3 \left(\frac{\alpha_u}{2} \|\mathcal{X}_u *_u \mathcal{Y}_u - \mathcal{C}\|_F^2 + \frac{\lambda}{2} (\|\mathcal{X}_u\|_F^2 + \|\mathcal{Y}_u\|_F^2) \right). \end{aligned}$$

Then \mathcal{C}^{t+1} is updated by

$$\begin{aligned}\mathcal{C}^{t+1} &= \underset{P_{\Omega}(\mathcal{C}-\mathcal{M})=0}{\operatorname{argmin}} \frac{1}{2} \left\| \sum_{u=1}^3 \alpha_u \mathcal{X}_u^t *_u \mathcal{Y}_u^t - \mathcal{C} \right\|_F^2 \\ &= \sum_{u=1}^3 \alpha_u \mathcal{X}_u^t *_u \mathcal{Y}_u^t + P_{\Omega} \left(\mathcal{M} - \sum_{u=1}^3 \alpha_u \mathcal{X}_u^t *_u \mathcal{Y}_u^t \right).\end{aligned}\tag{5}$$

Before we present how to update \mathcal{X}_u^{t+1} and \mathcal{Y}_u^{t+1} , we rewrite (4) as a corresponding matrix version. Denote $r_u := r_u(\mathcal{C})$, $r_u^l := r_u^l(\bar{\mathcal{C}}_u^{(l)})$ with $\bar{\mathcal{C}}_u^{(l)} \in \mathbb{C}^{n_{u_1} \times n_{u_2}}$, $u_1 < u_2$ and $u_1, u_2 \neq u$. Clearly, $r_u^l \leq r_u$ for all $l \in [\mathbf{n}_u]$. For each u and l , $\bar{\mathcal{C}}_u^{(l)}$ can be factorized as a product of two matrices $\hat{X}_u^{(l)}$ and $\hat{Y}_u^{(l)}$ of smaller sizes, where $\hat{X}_u^{(l)} \in \mathbb{C}^{n_{u_1} \times r_u^l}$ and $\hat{Y}_u^{(l)} \in \mathbb{C}^{r_u^l \times n_{u_2}}$ are the l /th block diagonal matrices of $\hat{X}_u \in \mathbb{C}^{n_{u_1} n_u \times \left(\sum_{l=1}^{n_u} r_u^l\right)}$ and $\hat{Y}_u \in \mathbb{C}^{\left(\sum_{l=1}^{n_u} r_u^l\right) \times n_u n_{u_2}}$. Let $\bar{X}_u^{(l)} = [\hat{X}_u^{(l)}, 0] \in \mathbb{C}^{n_{u_1} \times r_u}$, $\bar{Y}_u^{(l)} = [\hat{Y}_u^{(l)}, 0] \in \mathbb{C}^{r_u \times n_{u_2}}$ and \bar{X}_u, \bar{Y}_u be the block diagonal matrices with the l /th block diagonal matrices $\bar{X}_u^{(l)}, \bar{Y}_u^{(l)}$, respectively. Then $\hat{X}_u \hat{Y}_u = \bar{X}_u \bar{Y}_u$.

Together with Lemma 9, we have

$$\begin{aligned} \|\mathcal{X}_u *_{\mu} \mathcal{Y}_u - \mathcal{C}\|_F^2 &= \frac{1}{n_u} \|\bar{\mathcal{X}}_u \bar{\mathcal{Y}}_u - \bar{\mathcal{C}}_u\|_F^2 \\ &= \frac{1}{n_u} \|\hat{\mathcal{X}}_u \hat{\mathcal{Y}}_u - \bar{\mathcal{C}}_u\|_F^2 = \frac{1}{n_u} \sum_{l=1}^{n_u} \|\hat{\mathcal{X}}_u^{(l)} \hat{\mathcal{Y}}_u^{(l)} - \bar{\mathcal{C}}_u^{(l)}\|_F^2, \quad u \in [3]. \end{aligned}$$

Therefore, (4) can be rewritten as

$$\begin{aligned} \min_{\mathcal{C}, \mathcal{X}_u, \mathcal{Y}_u} \quad & \sum_{u=1}^3 \sum_{l=1}^{n_u} \left(\frac{\alpha_u}{2n_u} \left\| \hat{\mathcal{X}}_u^{(l)} \hat{\mathcal{Y}}_u^{(l)} - \bar{\mathcal{C}}_u^{(l)} \right\|_F^2 \right) \\ & + \sum_{u=1}^3 \sum_{l=1}^{n_u} \left(\frac{\lambda}{2n_u} \left\| \hat{\mathcal{X}}_u^{(l)} \right\|_F^2 + \frac{\lambda}{2n_u} \left\| \hat{\mathcal{Y}}_u^{(l)} \right\|_F^2 \right) \\ \text{s.t.} \quad & P_{\Omega}(\mathcal{C} - \mathcal{M}) = 0. \end{aligned} \tag{6}$$

To update $\hat{X}_u^{(I,t)}$, we consider its regularized version and have $\hat{X}_u^{(I,t+1)}$ as follows.

$$\begin{aligned}\hat{X}_u^{(I,t+1)} &= \underset{\hat{X}_u^{(I)}}{\operatorname{argmin}} \frac{\alpha_u}{2n_u} \left\| \hat{X}_u^{(I)} \hat{Y}_u^{(I,t)} - \bar{C}_u^{(I,t+1)} \right\|_F^2 + \frac{\lambda}{2n_u} \left(\left\| \hat{X}_u^{(I)} \right\|_F^2 + \left\| \hat{X}_u^{(I)} - \hat{X}_u^{(I,t)} \right\|_F^2 \right) \\ &= \left(\lambda \hat{X}_u^{(I,t)} + \alpha_u \bar{C}_u^{(I,t+1)} \left(\hat{Y}_u^{(I,t)} \right)^* \right) \left(\alpha_u \hat{Y}_u^{(I,t)} \left(\hat{Y}_u^{(I,t)} \right)^* + 2\lambda I \right)^{-1}.\end{aligned}\quad (7)$$

Similarly, $\hat{Y}_u^{(I,t+1)}$ can be updated by

$$\begin{aligned}\hat{Y}_u^{(I,t+1)} &= \underset{\hat{Y}_u^{(I)}}{\operatorname{argmin}} \frac{\alpha_u}{2n_u} \left\| \hat{X}_u^{(I,t+1)} \hat{Y}_u^{(I)} - \bar{C}_u^{(I,t+1)} \right\|_F^2 + \frac{\lambda}{2n_u} \left(\left\| \hat{Y}_u^{(I)} \right\|_F^2 + \left\| \hat{Y}_u^{(I)} - \hat{Y}_u^{(I,t)} \right\|_F^2 \right) \\ &= \left(\alpha_u \left(\hat{X}_u^{(I,t+1)} \right)^* \hat{X}_u^{(I,t+1)} + 2\lambda I \right)^{-1} \left(\lambda \hat{Y}_u^{(I,t)} + \alpha_u \left(\hat{X}_u^{(I,t+1)} \right)^* \bar{C}_u^{(I,t+1)} \right).\end{aligned}\quad (8)$$

Algorithm 3.1 Multi-Tubal Rank Tensor Completion (MTRTC)

Input: The tensor data $\mathcal{M} \in \mathbb{R}^{n_1 \times n_2 \times n_3}$, the observed set Ω , the initialized rank R^0 , parameters λ , ε and α_u , $u \in [3]$.

Initialization: \hat{X}_u^0 , \hat{Y}_u^0 , $u \in [3]$.

While not converge **do**

1. Fix \hat{X}_u^t and \hat{Y}_u^t to compute \mathcal{C}^{t+1} by (5).
2. Fix \hat{Y}_u^t and \mathcal{C}^{t+1} to update \hat{X}_u^{t+1} by (7).
3. Fix \hat{X}_u^{t+1} and \mathcal{C}^{t+1} to update \hat{Y}_u^{t+1} by (8).
4. Adopt the rank decreasing scheme to adjust $rank_{mt}(\mathcal{C})$ and adjust the sizes of \hat{X}_u^{t+1} and \hat{Y}_u^{t+1} .
5. Check the stop criterion: $\|\mathcal{C}_{\Omega}^{t+1} - \mathcal{M}_{\Omega}\|_F / \|\mathcal{M}_{\Omega}\|_F < \varepsilon$.
6. $t \leftarrow t + 1$.

end while

Output: \mathcal{C}^{t+1} .

Contents

- 1 Introduction
- 2 Multi-tubal rank: Definition and motivation
- 3 Tensor completion problem based on multi-tubal rank
- 4 Improvement with spatio-temporal characteristics
- 5 Numerical examples

In real world, some characteristics are included in some tensor data. For example, both the video data between two adjacent frames and the internet traffic data of two adjacent days have time stability. So we introduce three matrices F , G and H to adapt the data set in the following model

$$\begin{aligned} \min_{\mathcal{X}_u, \mathcal{Y}_u, \mathcal{C}} \quad & \sum_{u=1}^3 \frac{\alpha_u}{2} \|\mathcal{X}_u *_u \mathcal{Y}_u - \mathcal{C}\|_F^2 + \frac{\beta_1}{2} \|(\mathcal{X}_2 *_2 \mathcal{Y}_2) \times_1 F\|_F^2 \\ & + \frac{\beta_2}{2} \|(\mathcal{X}_3 *_3 \mathcal{Y}_3) \times_2 G\|_F^2 + \frac{\beta_3}{2} \|(\mathcal{X}_1 *_1 \mathcal{Y}_1) \times_3 H\|_F^2 \\ \text{s.t.} \quad & P_\Omega(\mathcal{C} - \mathcal{M}) = 0. \end{aligned} \tag{9}$$

Let $\beta_u = 0$ if there is no additional characteristics on the u th mode of \mathcal{C} . Hence, model (6) can be regarded as a special case of model (9).

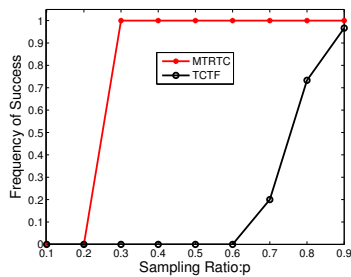
With Lemma 10, (9) can be rewritten as

$$\begin{aligned}
 & \min_{\mathcal{X}_u, \mathcal{Y}_u, \mathcal{C}} \quad \sum_{u=1}^3 \frac{\alpha_u}{2} \|\mathcal{X}_u *_u \mathcal{Y}_u - \mathcal{C}\|_F^2 + \frac{\beta_1}{2} \|\mathcal{F} *_2 (\mathcal{X}_2 *_2 \mathcal{Y}_2)\|_F^2 \\
 & \quad + \frac{\beta_2}{2} \|(\mathcal{X}_3 *_3 \mathcal{Y}_3) *_3 \mathcal{G}\|_F^2 + \frac{\beta_3}{2} \|(\mathcal{X}_1 *_1 \mathcal{Y}_1) *_1 \mathcal{H}\|_F^2 \\
 \text{s.t.} \quad & P_\Omega(\mathcal{C} - \mathcal{M}) = 0.
 \end{aligned} \tag{10}$$

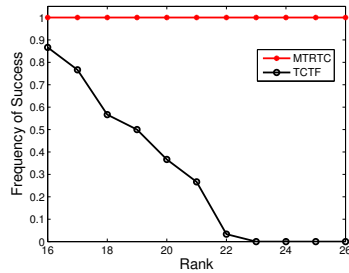
Contents

- 1 Introduction
- 2 Multi-tubal rank: Definition and motivation
- 3 Tensor completion problem based on multi-tubal rank
- 4 Improvement with spatio-temporal characteristics
- 5 Numerical examples

Numerical Simulation



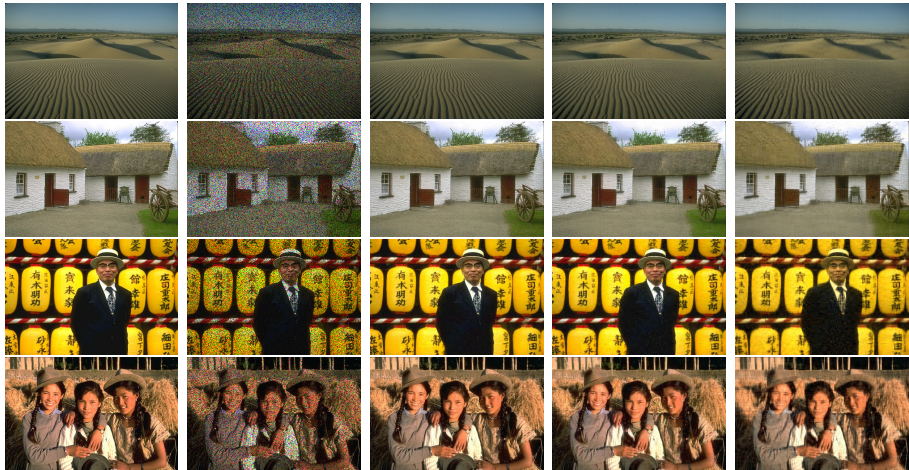
(a) Comparisons of different sampling ratios p



(b) Comparisons of different ranks

Figure: Comparisons between MTRTC and TCTF.

Image Simulation



Original

Observation

MTRTC

TCTF

TMac

Figure: Uniformly sampled image inpainting.

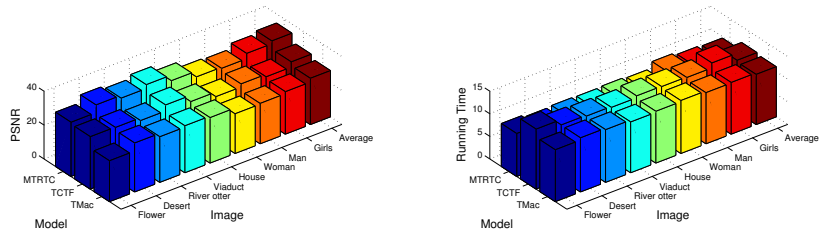
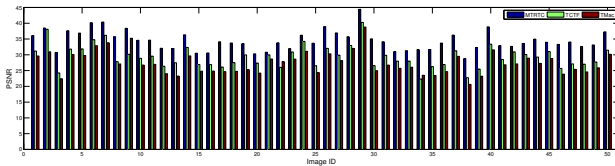


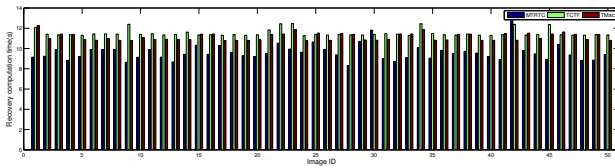
Figure: Comparisons of algorithms for the different Image.

Table: Numerical results for the different Image.

Image	MTRTC			TCTF			TMac		
	PSNR	RSE	time	PSNR	RSE	time	PSNR	RSE	time
Flower	32.07	0.079	9.51	30.95	0.090	13.28	24.09	0.199	11.47
Desert	36.61	0.031	9.02	30.72	0.060	12.08	28.96	0.074	12.00
River otter	34.95	0.052	9.23	29.08	0.102	11.89	26.95	0.131	11.67
Viaduct	37.23	0.031	9.11	32.63	0.053	11.69	27.74	0.093	11.24
House	33.88	0.038	9.26	28.91	0.067	12.11	26.89	0.084	11.48
Man	30.41	0.056	9.00	26.15	0.092	12.03	23.37	0.127	11.70
Human	29.80	0.064	10.41	27.97	0.079	11.91	23.84	0.127	11.31
Girl	32.92	0.049	9.88	26.49	0.103	12.99	25.12	0.121	11.46
Average	34.60	0.043	9.65	29.59	0.079	11.46	27.31	0.101	11.09



(a)



(b)

Figure: Comparisons of algorithms for the different Images.

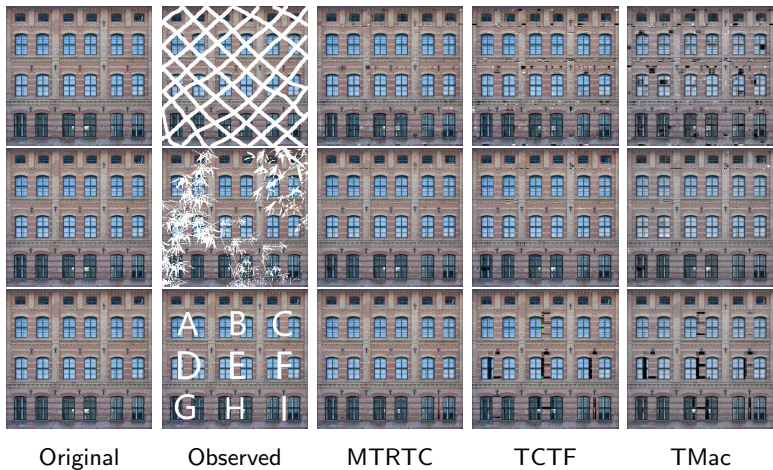


Figure: Recovered images of the masked images.

Table: Comparison on the PSNR and the RSE by MTRTC, TCTF and TMac.

Method	MTRTC		TCTF		TMac	
	PSNR	RSE	PSNR	RSE	PSNR	RSE
Grid	25.26	0.1048	22.57	0.1429	20.31	0.1854
Leaves	30.16	0.0596	28.69	0.0706	25.91	0.0972
Letters	30.82	0.0553	23.00	0.1359	21.70	0.1579

Video Simulation

The data between two adjacent frames of the video usually have not drastic change. To detect such stability, we calculate the data pairs of the corresponding positions between two adjacent frames. The difference for two adjacent frames of the video slots (k and $k + 1$) is defined as

$$\text{frame}(i, j, k) = |C_3^k(i, j) - C_3^{k+1}(i, j)|.$$

The smaller the $\text{frame}(i, j, k)$ is, the more stable the data between two adjacent frames of the video at frame k is. By computing the normalized difference values between two adjacent frames, we measure the stability between two adjacent frames of the video at frame k as

$$\Delta\text{gap}(i, j, k) = \frac{|C_3^k(i, j) - C_3^{k+1}(i, j)|}{\max_{1 \leq i \leq n_1, 1 \leq j \leq n_2, 1 \leq k \leq n_3 - 1} |C_3^k(i, j) - C_3^{k+1}(i, j)|}.$$

Here $\max_{1 \leq i \leq n_1, 1 \leq j \leq n_2, 1 \leq k \leq n_3-1} |C_3^k(i,j) - C_3^{k+1}(i,j)|$ means the maximal gap between any two adjacent frames of the video. We plot the CDF of $\Delta frame(i,j,k)$ in Figure 10. The X-axis represents the normalized difference values between two adjacent frames slots, i.e., $\Delta frame(i,j,k)$. The Y-axis represents the cumulative probability. We can see that the value $\Delta frame(i,j,k) < 0.6$ is more than 80%. These results indicate that the temporal stability exists in the real video data.

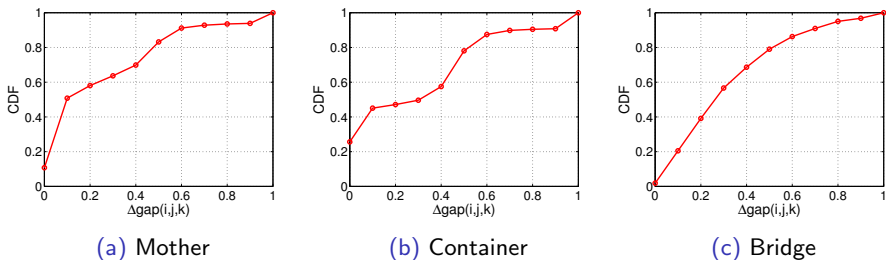


Figure: An empirical study of three sets of real video data.

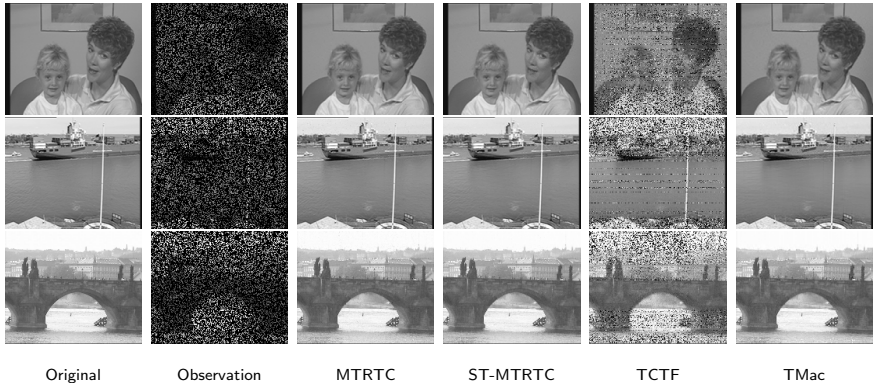
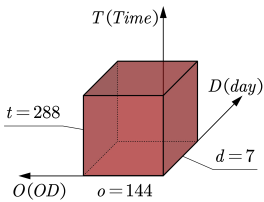


Figure: Examples of video inpainting.

Table: Numerical results of four algorithms on video recovery.

Method	Mother			Container			Bridge		
	PSNR	RSE	time	PSNR	RSE	time	PSNR	RSE	time
MTRTC	37.02	0.024	34.14	40.53	0.016	50.46	34.79	0.026	36.74
ST-MTRTC	37.79	0.022	46.33	42.58	0.012	60.63	35.55	0.024	33.37
TCTF	14.19	0.338	94.59	13.11	0.367	95.82	11.93	0.357	93.45
TMac	35.92	0.028	39.11	34.45	0.032	77.77	33.88	0.028	38.84

Internet Traffic Simulation

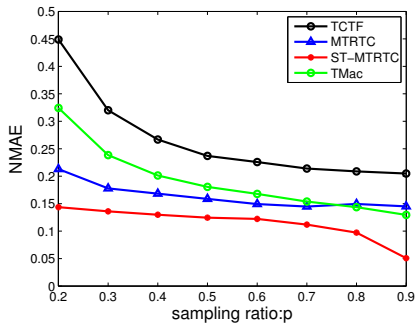


We model the traffic data as a third order tensor $\mathcal{M} \in \mathbb{R}^{D \times T \times O}$. Here O corresponds to the number of OD pairs with $O = N \times N$ (N is the number of nodes in the network), and there are D days to consider with each day having T time slots.

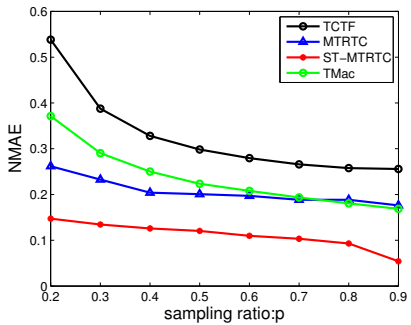
We use Abilene trace data¹ as an example to illustrate this model. The traffic data are collected between 144 OD pairs in 168 days, and the measurements are made every 5 minutes which corresponds to 288 time slots every day. We use a complete one week traffic data. Therefore, the trace data can be modeled as a third order tensor $\mathcal{M} \in \mathbb{R}^{7 \times 288 \times 144}$. We use the normalized mean absolute error (NMAE) in the missing values as a metric of the recovered data. The NMAE is defined as follows

$$\text{NMAE} = \frac{\sum_{(i,j,k) \notin \Omega} |\mathcal{M}_{ijk} - \hat{\mathcal{C}}_{ijk}|}{\sum_{(i,j,k) \notin \Omega} |\mathcal{M}_{ijk}|}.$$

¹<http://abilene.internet2.edu/observatory/data-collections.html>.



(a) the first week of data



(b) the second week of data

Figure: One sequence step with different sampling ratio.

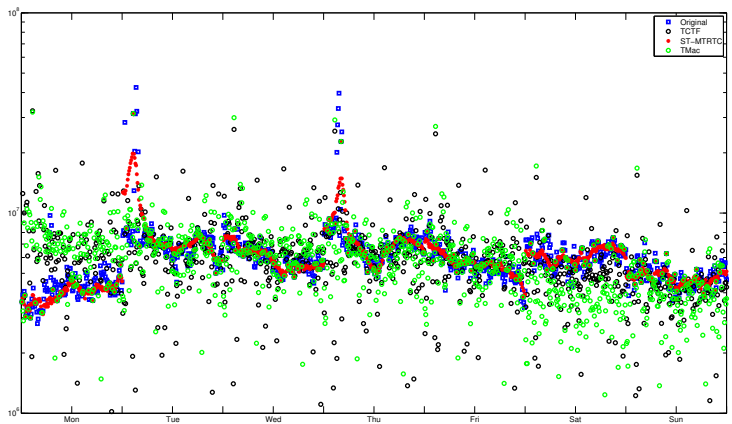


Figure: Sampling ratio $p = 0.2$.

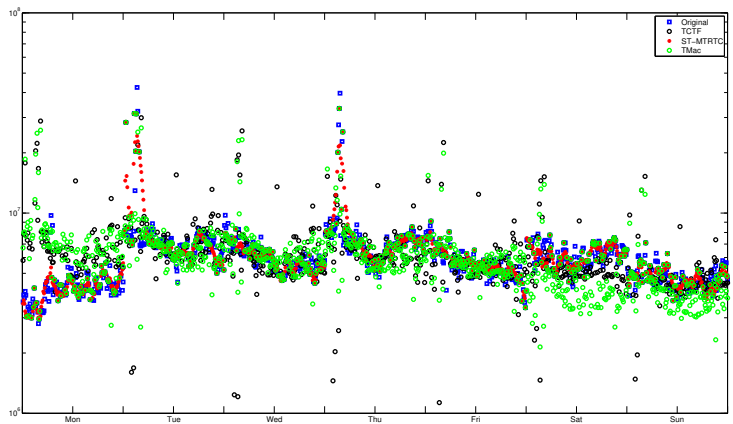


Figure: Sampling ratio $p = 0.4$.

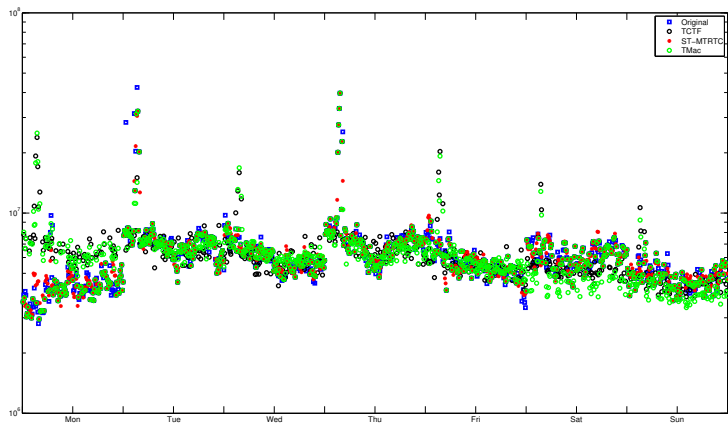


Figure: Sampling ratio $p = 0.6$.

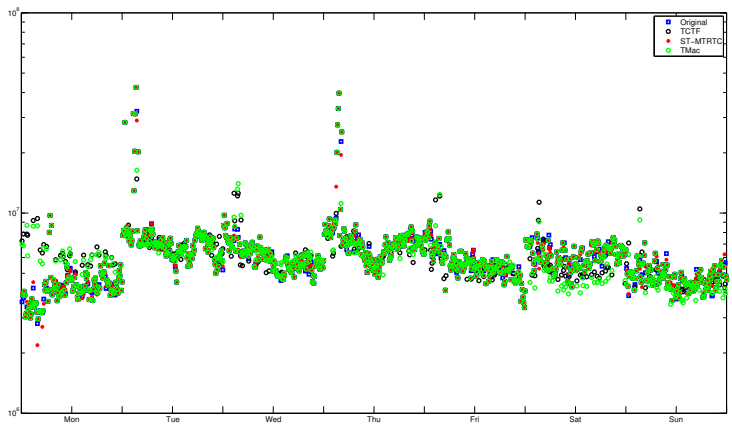


Figure: Sampling ratio $p = 0.8$.

Thank you!